



Standardisation of ^{241}Am activity for a key comparison

S. Pommé¹ · T. Altitzoglou¹ · R. Van Ammel¹ · G. Sibbens¹

Received: 12 July 2021 / Accepted: 23 August 2021 / Published online: 18 September 2021
© The Author(s) 2021

Abstract

The JRC applied six measurement techniques to standardise the activity of an ^{241}Am solution in the frame of the 2003 key comparison CCRI(II)-K2.Am-241. The methods used were alpha-particle counting at a defined small solid angle, high-efficiency particle and photon counting with a windowless 4π CsI(Tl) sandwich spectrometer, 4π alpha counting with a pressurised proportional counter, alpha-gamma coincidence counting and sum counting with a small pressurised proportional counter and a NaI(Tl) well detector, and 4π counting with a liquid scintillation counter. All results were consistent and an unusually low measurement uncertainty of 0.054% was achieved. An overview is presented of the outcome of the key comparison exercise, which demonstrates international equivalence.

Keywords Radionuclide metrology · Primary standardisation · Activity · Becquerel · Americium-241

Introduction

Through Key Comparisons, National Metrology Institutes (NMIs) with advanced measurement capabilities for accurate radioactivity measurements demonstrate international equivalence of their activity standards and contribute to a common definition of the SI-derived unit becquerel [1]. Unlike with other SI units, the becquerel needs to be defined individually for each radionuclide of interest, thus necessitating an array of measurement techniques to handle the largely differing decay schemes [2]. The workload is so extensive that no single NMI can standardise all relevant radionuclides, and even the combined effort from the international community has addressed only 72 nuclides through the International Reference System (SIR) [3, 4].

In the period 2002–2003, an unusually large amount of CCRI(II) key comparisons were held in which samples from a radioactive solution were distributed to NMIs and the results of their activity measurements were collected by the BIPM and directly compared [5]. Due to work overload, these standardisations were underreported in the literature and in the case of the 2003 CCRI(II)-K2.Am-241 exercise the summary ‘draft A’ report was never completed [6]. In

this paper, a summary is given of the six measurement techniques used at the JRC to standardise the activity per unit mass of ^{241}Am in solution. The methods used were alpha-particle counting at a small defined solid angle (α -DSA), high-efficiency particle and photon counting with a windowless 4π CsI(Tl) sandwich spectrometer ($4\pi\text{mix}$ -CsI), 4π alpha-particle counting with a pressurised proportional counter ($4\pi\alpha$ -LPPC), alpha-gamma coincidence counting ($4\pi\alpha - x,\gamma$ coinc) and sum ($4\pi\alpha + x,\gamma$ sum) counting with a small pressurised proportional counter and a NaI(Tl) well detector, and 4π counting with a liquid scintillation counter ($4\pi\text{mix}$ -LSC).

Some of the technical details are comparable to earlier published standardisation work on ^{238}Pu [7], ^{152}Eu [8], and ^{125}I [9], which may be used as additional source of information. The outcome of the JRC measurements are discussed and an informal comparison is made with the results obtained by various techniques at other NMIs on the basis of an overview graph in the ‘draft A’ stage and a table of the official ‘draft B’ combined results per NMI published in an overview report of ^{241}Am comparisons [6].

Decay scheme

Americium-241 decays by alpha transitions to ^{237}Np , emitting alpha particles with energy between 4.8 MeV and 5.6 MeV, in majority through two major transitions at

✉ S. Pommé
stefaan.pomme@ec.europa.eu

¹ European Commission, Joint Research Centre (JRC), Geel, Belgium

5.535 MeV ($P_{\alpha}=13.23\%$) and 5.578 MeV ($P_{\alpha}=84.45\%$) [10]. The decay product deexcites through emission of γ rays, conversion electrons, x rays, and Auger electrons. The two most intense γ rays have characteristic energies of 59.54 keV ($P_{\gamma+ce}=77.6$ (25)%, $\alpha_T=1.16$ (7), $I_{\gamma}=32.92$ (17)%) and 26.34 keV ($P_{\gamma+ce}=21$ (5)%, $\alpha_T=8$ (2), $I_{\gamma}=2.3$ (8)%) [10]. The gamma transitions have a significant probability of transferring their energy to one of the orbital electrons. The conversion electrons are ejected with a kinetic energy equal to the transition energy minus the electron binding energy, which for the 59.5 keV transition yields emissions from L electrons within 42 keV–47 keV and from higher shell electrons at 53.8 keV–59.5 keV [11]. Then follows a rearrangement of the atomic electron cloud, with emission of excess energy through a complex spectrum of x rays and Auger electrons. Auger electrons between 6 and 13.5 keV are emitted in about 33.4 (1.7)% of the ^{241}Am disintegrations. The DDEP (Decay Data Evaluation Project) recommended decay data were marginally different in 2003, but the results for most of the activity standardisation techniques do not crucially depend on modelling of the decay scheme [2, 12].

Sample preparation

Sources of ^{241}Am were prepared from the original solution supplied for the 2003 CCRI(II)-K2.Am-241 exercise, as well as from a dilution prepared gravimetrically at the JRC with a 6.1585 (1) dilution factor. For each source, an aliquot of the radioactive solution was deposited on the method-specific source substrate using the pycnometer method [13]. The weighing was done by mass substitution using a mass comparator (Mettler Toledo AT21 and AX26, Switzerland) with a set of weights traceable to the JRC standard kilogram which was directly traceable to the BIPM kilogram.

For all methods, except liquid scintillation counting, colloidal silica (1:10⁵ diluted Ludox, DuPont de Nemours&Co, USA) was deposited on the source substrate as a seeding agent before the aliquot, typically 15–20 mg of the active solution, was deposited and dried. The evaporation process was accelerated by employing a special source-drying device using hot jets (50 °C) of dry nitrogen [14]. Source preparation was done in a clean environment to minimise inclusion of dust and foreign particles and the sources were placed in desiccators immediately after drying. Optimal source quality was thus achieved through a homogeneous spread of small crystals resulting in less energy loss of the emitted alpha particles inside the source material.

For measurements in gas counters, 24 sources were prepared on 35 $\mu\text{g cm}^{-2}$ VYNS foils (polyvinylchloride-polyvinylacetate copolymer), coated on both sides with 16.6 $\mu\text{g cm}^{-2}$ Au and mounted on rings with 34/22 mm

outer and inner diameter, respectively. Additionally, 5 sources were prepared on 20 $\mu\text{g cm}^{-2}$ VYNS foils, coated on both sides with 15 $\mu\text{g cm}^{-2}$ Au and mounted on rings with 55/35 mm outer and inner diameter, respectively. About an equal number of sources was made from the original (14) and diluted (15) solution.

Special source supports were used for the CsI(Tl) sandwich spectrometer: Mylar foils with a thickness of 3.2 μm were stretched in between solid brass rings. A hole of 10 mm diameter was punched into the centre of the foil, which was then covered with a VYNS foil of 35 $\mu\text{g cm}^{-2}$. Ten ^{241}Am sources were produced, of which 3 from the original solution and 7 from the dilution.

Polished glass discs were used as source supports in the DSA α -particle counter. The cleaning procedure commenced with wiping with acetone and tissue, then 20 min in ultrasonic bath with diluted HNO_3 at 50 °C, then 20 min with diluted NH_4OH at 50 °C, and then four times 10 min in deionised water at 50 °C. Of the 10 sources for alpha-particle counting at a defined solid angle, 7 were from the original solution and 3 from the dilution.

For liquid scintillation counting (LSC), the radioactive solution was dispensed directly into the LSC vials containing the LS cocktail. Two types of cocktail were used in either 20 ml Packard High Performance (low-potassium) glass or Low-diffusion polyethylene vials: 18 sources were prepared in 15 ml Ultima Gold + 1 ml H_2O and 13 sources in 10 ml Ultima Gold AB. The amount of (original) radioactive solution in the samples ranged from 2.6 to 46 mg. There were in total 16 sources from the original solution and 15 from the dilution. Four additional sources in 15 ml InstaGel Plus were not included in the reported result.

Blank samples were prepared in the same way as the active sources, but without the addition of radioactive solution. The radiopurity of the ^{241}Am solution was verified with γ -ray and α -particle spectrometry [15] measurements and no impurities were detected. The emptied ampoule of the solution was checked for activity adsorbed in the glasswork: it was rinsed twice with 1 ml 2 N HCl and once with 1 ml H_2O , then measured by liquid scintillation counting. Assuming 50% of the normal detection efficiency, the measured residual activity was of the order of 0.001% of the total activity, and this was taken into account in the uncertainty budget.

4 π CsI(Tl) sandwich spectrometer

The windowless 4 π CsI(Tl) sandwich spectrometer, designed by Denecke [16] at the JRC, consists of two CsI(Tl) scintillation crystals, mounted on a source-interlock chamber (Fig. 1). The chamber interior is continuously flushed with dry hydrogen to protect the hygroscopic CsI(Tl) crystals from contact with humidity in the air. The source is



Fig. 1 The 4π CsI(Tl) sandwich spectrometer with surrounding lead shield. Designer of the instrument, Bruno Denecke, holding a bespoke source support



Fig. 2 Shape of a CsI(Tl) crystal (51 mm diameter, 25 mm height) with a semi-spherical cavity in its surface that will surround the radioactive spot

sandwiched between the front faces of the crystals, which have a semispherical cavity each to avoid physical contact with the active material (Fig. 2). Because of the spherical cavity, all radiations enter the scintillation crystals perpendicularly, reducing the influence of the dead layer. The detector is sensitive to alpha and beta particles, as well as x rays and gamma rays. It is limited at the low-energy side—up to about 10 keV—due to electronic noise and at the high-energy side—above a few hundreds of keV—due to partial transparency to photons. The instrument is unique among standardisation laboratories, in spite of its unparalleled quality to detect the decay of radionuclides with complex decay schemes at an efficiency close to unity. The latter was demonstrated in key comparisons of ^{152}Eu , ^{192}Ir , and $^{166\text{m}}\text{Ho}$ [5].

A block diagram of the electronics is shown in Fig. 3. An advanced live-time technique is used to compensate for count loss due to system dead time [17, 18], however not including a secondary correction for cascade effects of

pileup [19] with dead time [20]. The pulses of the top and bottom channels of the sandwich spectrometer are summed at the output of the amplifier system composed of photoelectron multipliers and pulse-shaping amplifiers. A threshold discriminator followed by a retriggerable dead time generator of the extending type ($\tau_1 = 51.20$ (2) μs) with a zero-recovery time and a live-time gate are used. Subsequent scalers record the event rate and live-time clock pulses. Another chain with non-extending dead time ($\tau_2 = 51.50$ (2) μs) was run in parallel. An additional non-extending dead time of 1 ms is triggered by unusually high pre-amplifier pulses, thus eliminating cosmic showers and occasional electronic interference. In parallel, a multichannel analyser system is used for spectral inspection and visualisation of the low-energy threshold. For redundancy, also the ADC busy time period is processed by a live-time gate.

The $4\pi\text{mix-CsI}$ counting method is akin to $4\pi\gamma$ counting with NaI(Tl) well detectors [21], except that the counting efficiency for particles adds significantly to the total detection probability. At that time, no dedicated software like STEFFY [22–25] or Monte Carlo routines were used for the efficiency calculation. The detection inefficiency was estimated at 0.03%, since the chance is low that no detectable pulse per decay is generated by the alpha particle, gamma rays, x rays, or secondary electrons. Nevertheless, an uncertainty of 0.1% was assigned to this non-efficiency component (considering also a 4 μm separation gap between the crystal faces, which reduces the solid angle of detection). Since the threshold was set at 15 keV, an additional mass-dependent correction of 0.01%–0.2% had to be made for extrapolating the low-energy tailing of the spectrum to zero energy. An example is shown in Fig. 4. This led to the second largest uncertainty component of 0.06%. The third significant contribution of 0.05% came from weighing [26], based on an estimate of about 0.12% uncertainty per source. The background rate was 4.3 s^{-1} , accounting to a 0.1%–1% correction, and the imposed dead time was 2–20% at count rates of 500–5000 s^{-1} . Uncertainty propagation of the half-life is negligible [27, 28]. The combined total uncertainty on the ^{241}Am activity concentration was 0.13%.

4π large pressurised proportional counter

The 4π Large Pressurised Proportional Counter (LPPC) consists of a cylindrical gas chamber and a central planar cathode dividing it into two D-shaped counters with an anode wire each, as described in detail elsewhere [29] (Fig. 5). The source is integrated in the cathode, and the VYNS foil has been made conductive with an evaporated gold layer on both sides (even though one side would have sufficed). The counting gas (90% argon, 10% methane) was continuously refreshed, while being kept at a constant pressure of 0.8 MPa

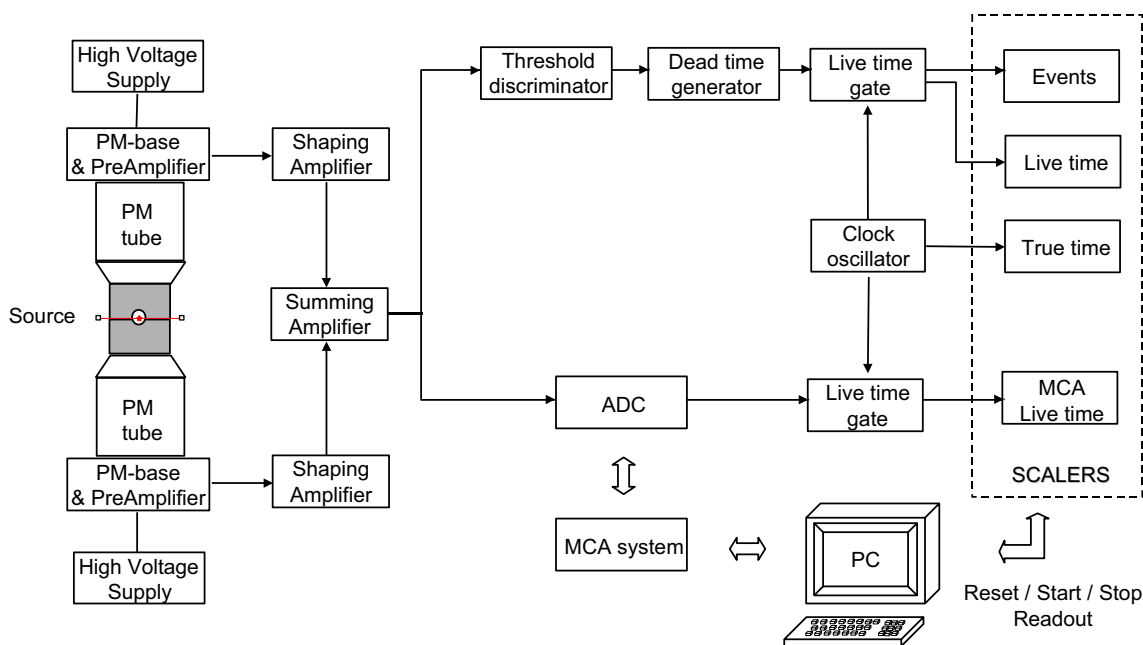


Fig. 3 Block diagram of the electronic pulse processing system of the CsI(Tl) sandwich spectrometer (PM=photomultiplier, ADC=analog-to-digital converter, MCA=multi-channel analyser)

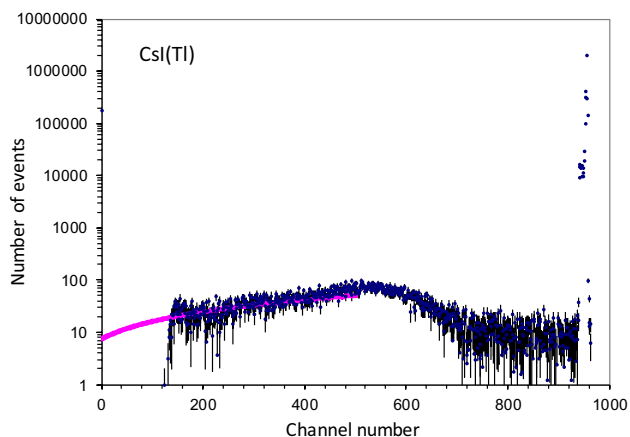


Fig. 4 Pulse-height spectrum of the diluted source Am²⁴¹C0322 in the CsI(Tl) sandwich spectrometer. The high-energy pulses are limited in amplitude by electronic termination. The threshold of the single-channel counter is at channel 150 and the missing counts below the threshold, about 0.06% of the total spectrum, are estimated by extrapolation of the spectral shape to the origin

[30]. The discrimination level was set at 0.55 MeV, aiming at detecting exclusively the alpha particles emitted from the ²⁴¹Am decay. In total, 22 sources were measured with count rates varying from 600 to 5000 s⁻¹. The background rate was of the order of 1 s⁻¹. A non-extending dead time of $\tau = 20.72 \mu\text{s}$ was imposed on every counted event, resulting in 0.5%–22% dead time.

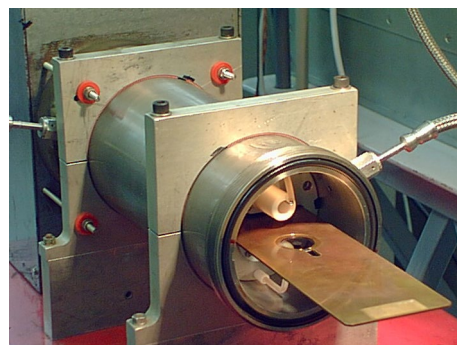


Fig. 5 Inside view of the large pressurised proportional counter with a radioactive source integrated in the central cathode plate and the connectors of the anode wires at high voltage. The LPPC can be hermetically closed to run a continuous flow of counting gas, kept in dynamic equilibrium with an external reference pressure vessel by actively controlling the gas outflow

The major correction was due to self-absorption of the alpha particles inside the source material and substrate (VYNS + gold). This contribution was examined by performing additional measurements after covering the sources with an extra foil of the same composition and thickness. A calculation was made of the expected fraction of alpha particles absorbed in the source, by determining the range of the particles in the composition of the source materials (Am, CH₂H₃Cl, C₁₀H₈O₄, Au) [31]. For each layer, the ratio was calculated between the layer thickness and the alpha-particle range, and a summed value of 0.0094 was

derived. This means that particles emitted within an angle of $\theta = \text{asin}(0.0094)$ to the plane of the foil would be blocked, which corresponds to a loss of $\cos(\pi/2 - \theta) - \cos(\pi/2) = 0.94\%$. The counting efficiency was corrected by 0.47% for particle loss in a source and by 0.94% when the source was covered with an extra foil on top. Good consistency was reached among all types of sources, covered or uncovered, on large or small diameter source support, made from drops of the original or diluted solution.

An uncertainty of 0.2% was assigned to the self-absorption correction, and in the same order of magnitude, 0.21% was attributed to the extrapolation of the energy spectrum to compensate for the non-recorded fraction of events below the discrimination level (Fig. 6). This resulted in a combined uncertainty of 0.3%.

4 π - α, γ coincidence counting

The coincidence method [32–35] offers an alternative to high-efficiency methods for radionuclides which emit at least two distinguishable types of radiation in their decay process; In the case of ^{241}Am decay, the alpha particles are followed by the emission of photons from the deexcitation of the decay product. The detection set-up consists of two detectors which, ideally, are exclusively sensitive to one type of radiation: a small version of the pressurised gas proportional counter (SPPC) as the particle detector and a 15 cm \times 15 cm NaI(Tl) well crystal as the photon detector (Fig. 7). The SPPC is operated with the same gas and pressure regulation system as the LPPC. The source is placed in the cathode of the SPPC, which is then slid inside the 50 mm diameter well of the NaI detector. This ensures a favourable geometry and high detection efficiency for both detectors.

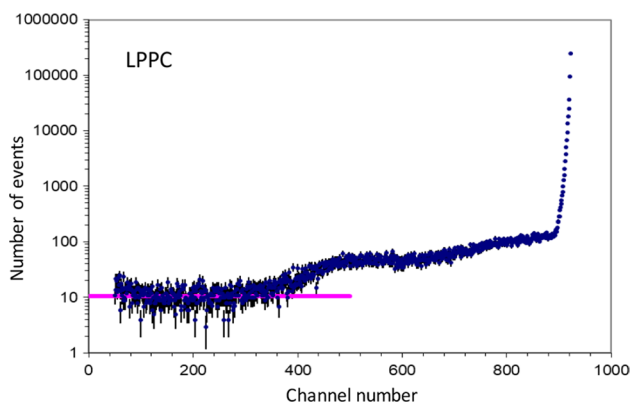


Fig. 6 Pulse-height spectrum of alpha particles measured with the LPPC, and extrapolation of the missing 0.21% fraction of counts below the energy threshold for the diluted source Am241V0336. Sources from the original solution generally have a larger tailing fraction (e.g. of the order of 0.4%)

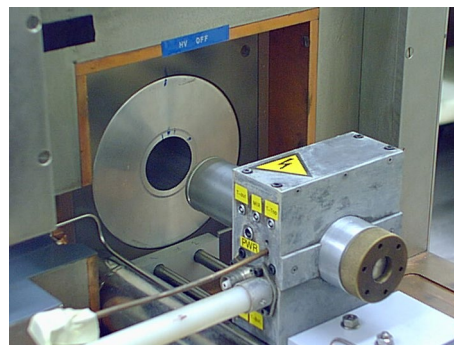


Fig. 7 Coincidence counting set-up comprising a small pressurised proportional counter (SPPC) as particle detector, which fits inside the well of a large NaI(Tl) scintillation crystal acting as photon detector

The particularity of the coincidence method comes from the additional counting channel that records the number of coincident events in both detectors. In an ideal situation, the source activity and both detector efficiencies can be directly derived from the two detector count rates and the coincidence rate. In practice, the activity is obtained from a linear extrapolation of a series of measurements performed at varying counting inefficiencies approaching zero. The signal processing can be done by classical electronics [33] as well as by digital means [34]. Live-time counting is applied to the individual detector channels, whereas the classical method relies on dedicated formulas for the combined dead time in the coincidence channel, depending on the type of imposed dead time [32]. Cascade effects [20] have been neglected in the assumption that they somewhat cancel out when taking the ratio of the individual and coincident count rates.

The energy thresholds were set at more than 200 keV in the SPPC and 2 keV in the NaI(Tl) detector. The corresponding imposed non-extending dead times were $\tau_1 = 8.62$ (2) μs and $\tau_2 = 9.11$ (2) μs , the coincidence resolving times $\tau_{R1} = 0.225$ (5) μs and $\tau_{R2} = 1.50$ (1) μs , with a delay of the particle channel of $\delta\alpha = 0.50$ (5) μs (assessed from a digital scope). The sum of the resolving times is smaller than the dead times, but exceeds the width of the time difference distribution of both channels. The maximum particle counting efficiency achieved was 99.45% and extrapolation was performed by electronically varying the threshold level. The results were perfectly linear over a wide range and the slope was negligible compared to the small inefficiencies that could be reached for each source, $(1 - \epsilon_\alpha)/\epsilon_\alpha < 0.015$, such that the activity could even be derived on the basis of a single measurement. The results from 18 sources showed a standard deviation within 0.4% and a total uncertainty of 0.10% was assigned to the mean. The data spread mostly reflects the combined uncertainties from weighing and counting statistics.

4 π - α , γ sum counting

Using the same SPPC and NaI(Tl) set-up as for the coincidence measurements, the signals can be analysed alternatively as a summing experiment. For each of 18 sources, only measurements with 99.0–99.5% efficiency in the particle detector were collected. Thus, the correction for the missing 0.5%–1% of the decay rate could be obtained directly from the count rate in the photon detector minus the coincident counts, to avoid double counting. The results were the same for sources covered with an extra foil. The uncertainty of the method was marginally larger (0.11%) than for the coincidence method. Both methods are highly correlated, but independence was simulated by applying a slightly increased uncertainty on the extrapolations.

α -counting at a defined solid angle

Since energy loss of alpha particles in a solid source is problematic at the smallest emission angles, accuracy can be gained by counting particles emitted perpendicular to the source plane in a counter with a well-defined small solid angle (DSA) [36]. The JRC has two α -DSA set-ups consisting of a source chamber, distance tube, and a circular diaphragm in front of a large PIPS detector [37]. Variations in geometrical efficiency can be realised by replacing diaphragms and distance tubes. Accurate measurements of the distance between source and diaphragm as well as the diaphragm radius were performed by optical techniques [37, 38], which have later been replaced by a 3D-coordinate measuring machine [39]. The solid angle subtended by the detector can be addressed with exact mathematical algorithms for circular and elliptical configurations [40, 41], however the method gains significant robustness by taking into account the source activity distribution [36, 42, 43]. A relative uncertainty of 0.1% can be reached.

In the first counter, α -DSA1, a solid angle of 1.9% of 4π sr was obtained with a 30.019 mm diameter diaphragm (and a 1200 mm² PIPS detector) at a distance of 52.1 mm from the source. In the second counter, α -DSA2, two configurations were constructed: 0.77% of 4π sr with a 53.856 mm diameter diaphragm (and a 3000 mm² PIPS detector) at a distance of 151.5 mm; and 0.88% of 4π sr with a 19.999 mm diameter diaphragm (and a 450 mm² PIPS detector) at a distance of 52.0 mm. The intrinsic detection efficiency of the PIPS detectors was assumed to be 100%. For each source, the activity distribution was determined by autoradiographs and the average source substrate thickness was determined individually to improve the precision of the distance measurement [37, 38, 43]. This was an important correction to the solid angle calculation, since autoradiographs obtained

with a phosphor imaging screen showed a significant variation in the radial distribution of the source activity (Fig. 8). The source preparation procedure for alpha-emitter sources was later optimised to improve homogeneity by pretreating the substrates with wetting and seeding agents using an airbrush [44].

The block diagram in Fig. 9 represents the standard data acquisition for decay counting at the JRC. The output signal

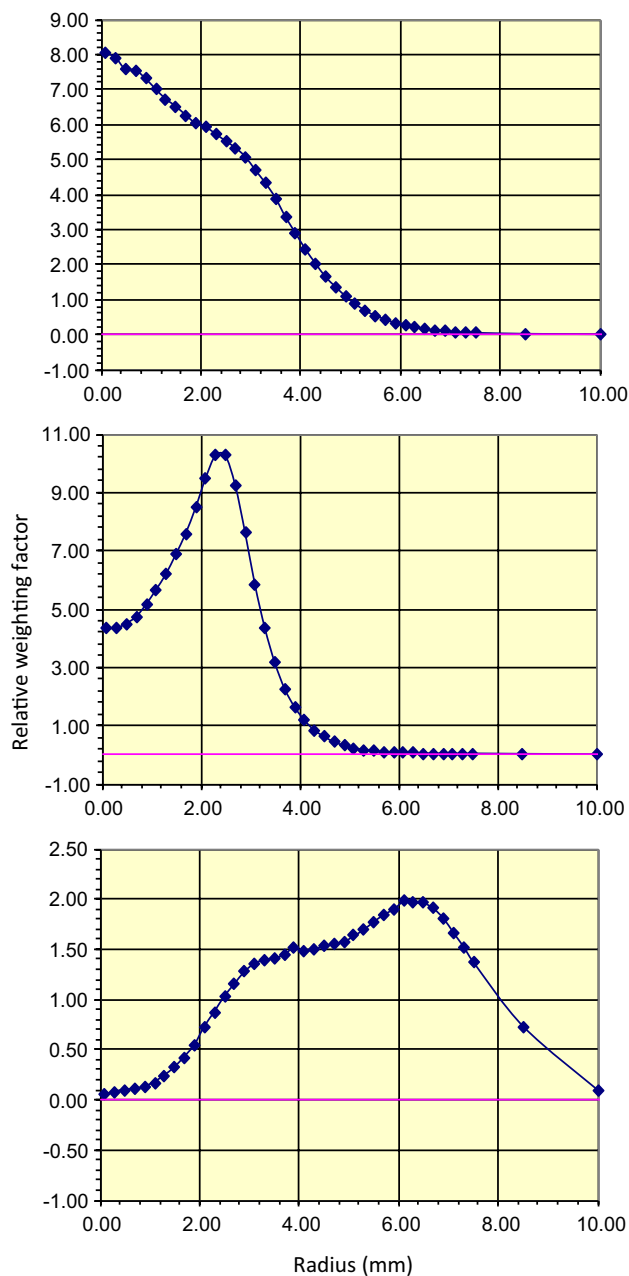


Fig. 8 Relative weighting factors to account for the activity distribution derived from autoradiographs in three sources. A perfectly homogeneous, centred source would show a rectangular distribution, whereas the real drop-deposited sources showed concentrations in the centre (top), middle (middle), or outer rim (bottom)

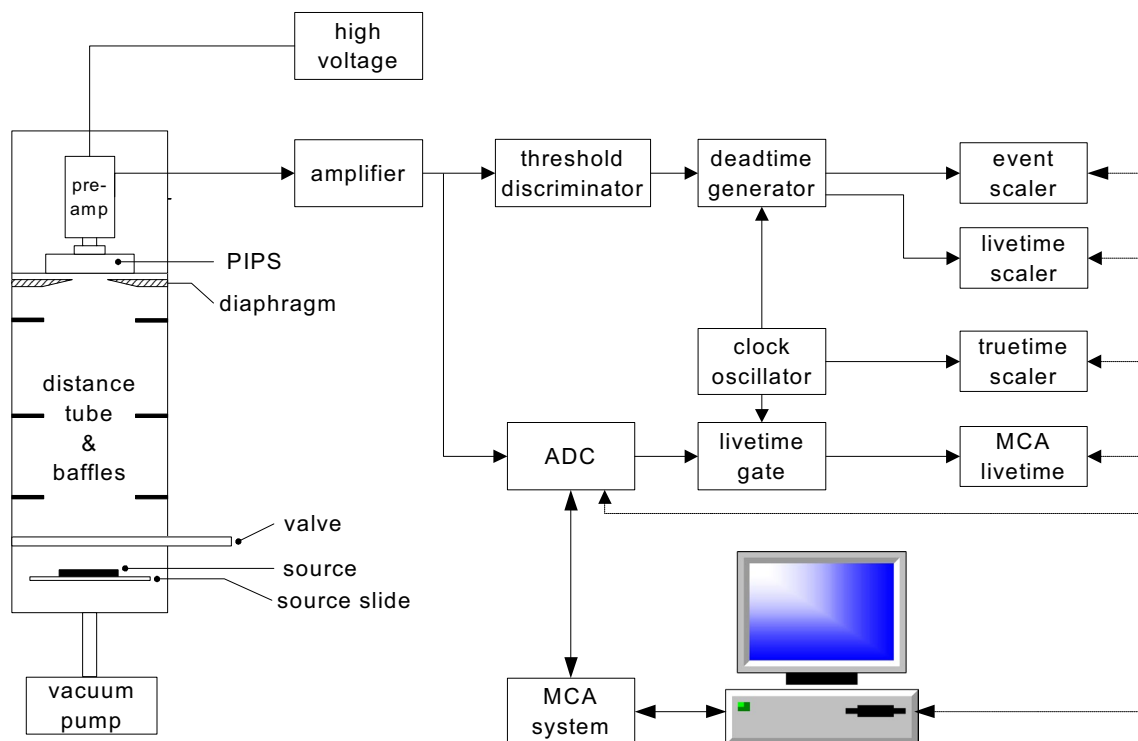


Fig. 9 Block diagram of the electronic pulse processing system of an alpha counter at a defined small solid angle (ADC = analog-to-digital converter, MCA = multi-channel analyser). A similar scheme was used for the LPPC

from the PIPS detector is amplified and then processed in parallel by a multichannel analyser (MCA) and a single channel (SC) counter. The SC branch of the system consists of an adjustable threshold discriminator, succeeded by a non-extending dead-time generator of zero recovery time and a live-time clock gate (LGN), which processes the system clock pulses and establishes the live-time of the measurement. The MCA consists of an Analog-to-Digital Converter (ADC) and a PC resident Multi-Channel Acquisition board (MCA) which accumulates the pulse-height distribution of the detected nuclear events. The MCA spectrum is used to estimate the fraction below the threshold of the SC branch (Fig. 10).

A stable quartz oscillator (QC 100 kHz/100 Hz generator, JRC-Geel) with a frequency of 100 kHz provides the time base to the live-time clock gates. The quartz oscillator delivers also a 100 Hz-clock signal used as the true-time clock. The live-time clock pulses are electronically divided by 1000 after passing the live-time clock gates. As a result, all time counts have a resolution of 10 ms. A PC-resident array of eight scalers is used to accumulate all event pulses and clock pulses generated in the system. The scalers count the live time and true time along with the event detections, so that a correction for dead time can be made for each measurement. The busy-period signals from the MCA are processed by the second live-time clock gate of the same LGN unit.

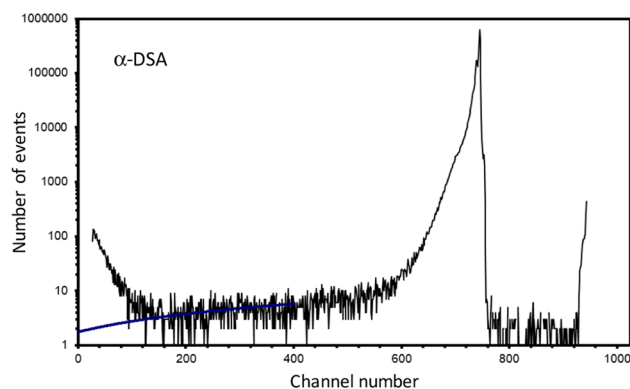


Fig. 10 Extrapolation of the DSA alpha pulse-height spectrum to zero energy. The fraction below threshold level is of the order 0.01%

This redundant count rate is used as a check value only. The clock of the PC is synchronised to coordinated universal time (UTC).

4 π liquid scintillation counting

The 4 π liquid scintillation measurements were performed using a Packard Tri-Carb model 3100 TR/AB (PerkinElmer, Inc., Waltham, MA, USA) and a Wallac Quantulus 1220 (PerkinElmer, Inc.) liquid scintillation spectrometer. Both

instruments were operated with two phototubes in sum-coincidence mode at a temperature of about 12 °C. All samples were measured 10 times, for 10 min each, with the Packard LSC and 5 times, for 10 min each, using the Quantulus LSC, over a period of 3 months. Rate-related count loss was corrected for by the built-in dead-time compensation systems of the instruments. The background count rates for the Packard and the Quantulus were 0.6 s^{-1} and 0.3 s^{-1} for the samples in glass vials and 0.3 s^{-1} and 0.1 s^{-1} for the samples in PE vials, respectively. The results were calculated in the assumption that the counting efficiency for alpha-particle emitters is 100%. A 0.2% uncertainty on the counting efficiency was included in the uncertainty budget. There was a 0.34% discrepancy between both instruments, with the Quantulus LSC giving the lower result. Half of that discrepancy (0.2%) was added to the uncertainty budget as

instrument-dependent uncertainty. An overall uncertainty of 0.4% on the ^{241}Am activity per unit mass was reported.

Measurement results

An overview of the ^{241}Am activity concentration results with six standardisation techniques is shown in Fig. 11 and the associated uncertainty budgets are collated in Table 1. The standard deviation of the data set (0.033%) is smaller than the propagated uncertainty of the mean (0.054%). Having demonstrated confidence in the uncertainty estimates, the final result was calculated from an inverse-variance weighted mean. This is equivalent to the Power-Moderated-Mean (PMM) [45–48] with power $\alpha=2$, since $\chi^2=0.59 < 1$ and therefore no common uncertainty component is added to the data set. The strong coherence of the measurement results confirms once again the absence of a significant bias in any of these methods. Redundancy of measurement techniques is an extremely important tool for a standardisation laboratory to gain confidence in its methods. The next level is through demonstration of equivalence with other laboratories through a large-scale comparison.

In Table 2, an overview is presented of the reported results from NMIs participating in the 2003 CCRI(II)-K2. Am-241 key comparison exercise, i.e. the (unofficial) results obtained with different standardisation techniques and the final (official) mean value assigned by the NMIs. In this paper, a reconstruction is made on the basis of three pieces of information: (1) an anonymised preliminary graphics file containing most of the measurement results by different methods obtained from BIPM through a private communication, (2) a more official version of the graph in pdf format

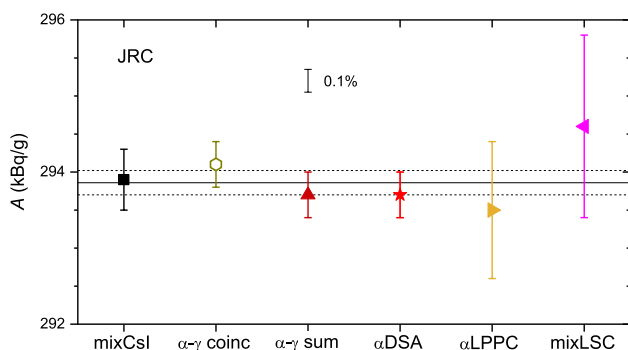


Fig. 11 Overview of the ^{241}Am activity per unit mass values and their standard uncertainty obtained with six primary standardisation techniques in the Radionuclide Metrology laboratory of the JRC in Geel. All results are consistent with the weighted mean value and its standard uncertainty, represented by the lines

Table 1 Standard relative uncertainty estimates (expressed in %) associated with the ^{241}Am activity concentration results obtained with six standardisation techniques at the JRC

| Uncertainty component | CsI | α - γ coinc | α - γ sum | α DSA | LPPC | LSC |
|-----------------------|--------|---------------------------|-------------------------|--------------|--------|--------|
| Counting statistics | 0.01 | 0.05 | 0.05 | 0.02 | 0.05 | 0.1 |
| Weighing | 0.05 | 0.05 | 0.05 | 0.05 | 0.05 | 0.2 |
| Dead time | 0.02 | 0.02 | 0.02 | 0.02 | 0.02 | 0.1 |
| Background | <0.01 | <0.01 | <0.01 | <0.01 | <0.01 | 0.0025 |
| Counting time | <0.001 | <0.001 | <0.001 | <0.001 | <0.001 | 0.05 |
| Resolving time | | <0.01 | <0.01 | | | |
| Gandy effect | | 0.01 | 0.01 | | | |
| Adsorption | 0.002 | 0.002 | 0.002 | 0.002 | 0.002 | 0.002 |
| Half-life | <0.001 | <0.001 | <0.001 | <0.001 | <0.001 | <0.001 |
| Self-absorption | 0.10 | | | | 0.20 | |
| Extrapolation | 0.06 | 0.07 | 0.07 | 0.01 | 0.21 | |
| Detection efficiency | | | | 0.08 | | 0.2 |
| Instrument dependence | | | | | | 0.2 |
| Sample stability | | | | | | 0.1 |
| Wall effect | | | | | | 0.1 |
| Total | 0.13 | 0.10 | 0.11 | 0.10 | 0.3 | 0.4 |

Table 2 Results of the CCRI(II)-K2. Am-241 comparison for each participating laboratory (indicated in bold) and individual results per method extracted from two versions of the ‘draft A’ plot. Uncertainty values may vary slightly through rounding effects

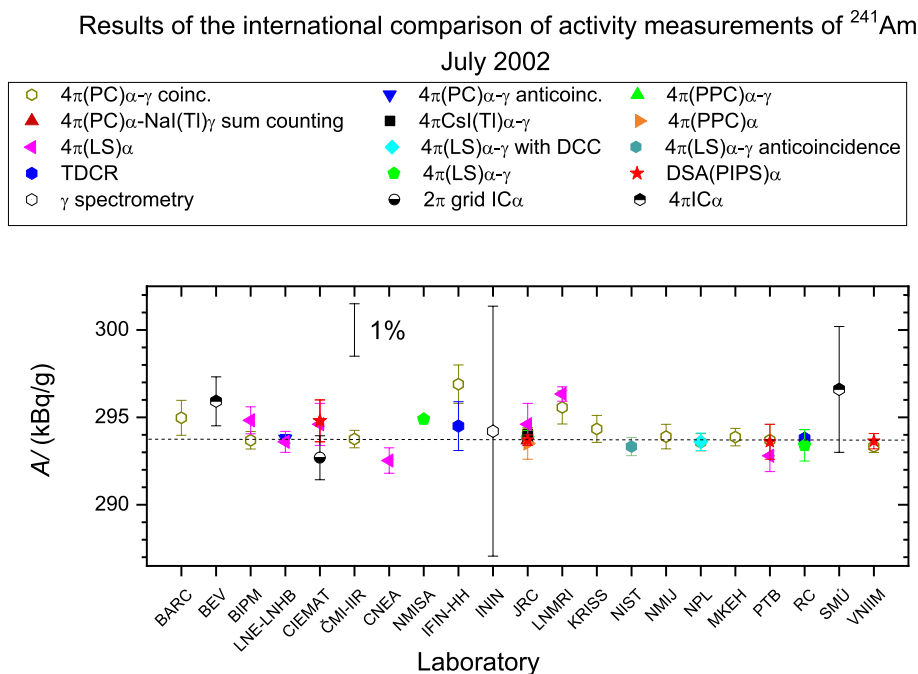
| | Laboratory Method | Activity per unit mass (kBq g ⁻¹) | Standard uncertainty (kBq g ⁻¹) | Relative uncertainty (%) | Zeta score (-) |
|----|------------------------|---|---|--------------------------|----------------|
| | Power-moderated mean | 293.75 | 0.10 | 0.032 | 0.0 |
| 1 | BARC | 294.97 | 1.0 | 0.34 | 1.2 |
| | 4π(PC)α-x,γ coinc | 294.97 | 1.0 | 0.34 | |
| 2 | BEV ^(a) | 295.92 | 1.4 | 0.47 | 1.6 |
| | 4πx,γ-IC | 295.92 | 1.4 | 0.47 | |
| 3 | BIPM | 294.03 | 0.53 | 0.18 | 0.5 |
| | 4π(PC)α-x,γ coinc | 293.69 | 0.50 | 0.17 | |
| | 4πmix-LSC | 294.83 | 0.77 | 0.26 | |
| 4 | CIEMAT | 294.07 | 0.71 | 0.24 | 0.5 |
| | 4πmix-LSC | 294.6 | 1.2 | 0.41 | |
| | α-DSA-PIPS | 294.8 | 1.2 | 0.41 | |
| | 2πα-grid IC | 292.69 | 1.26 | 0.43 | |
| 5 | ČMI-IIR | 293.76 | 0.50 | 0.17 | 0.0 |
| | 4π(PC)α-x,γ coinc | 293.76 | 0.50 | 0.17 | |
| 6 | CNEA | 292.53 | 0.73 | 0.25 | -1.7 |
| | 4πmix-LSC | 292.53 | 0.73 | 0.25 | |
| 7 | IFIN-HH ^(b) | 296.9 | 1.1 | 0.36 | 2.9 |
| | 4π(PC)α-x,γ coinc | 296.9 | 1.1 | 0.36 | |
| | TDCR | 294.5 | 1.4 | 0.48 | |
| 8 | ININ ^(a) | 294.2 | 7.1 | 2.4 | 0.1 |
| | γ-ray spectrometry | 294.2 | 7.1 | 2.4 | |
| 9 | JRC | 293.86 | 0.16 | 0.054 | 0.9 |
| | 4πα-LPPC | 293.5 | 0.9 | 0.30 | |
| | 4π(PC)α-x,γ coinc | 294.1 | 0.3 | 0.10 | |
| | 4π(PC)α-x,γ sum | 293.7 | 0.3 | 0.11 | |
| | 4πmix-LSC | 294.6 | 1.2 | 0.4 | |
| | 4πmix-CsIS | 293.9 | 0.4 | 0.13 | |
| | α-DSA-PIPS | 293.7 | 0.3 | 0.10 | |
| 10 | KRISS | 294.2 | 0.8 | 0.27 | 0.6 |
| | 4π(PC)α-x,γ coinc | 294.2 | 0.8 | 0.27 | |
| 11 | LNE-LNHB | 293.77 | 0.24 | 0.08 | 0.1 |
| | 4π(PC)α-x,γ anticoinc | 293.77 | 0.24 | 0.08 | |
| | 4πmix-LSC | 293.6 | 0.6 | 0.20 | |
| 12 | LNMRI ^(b) | 296.25 | 0.33 | 0.11 | 7.4 |
| | 4π(PC)α-x,γ coinc | 295.57 | 0.95 | 0.32 | |
| | 4πmix-LSC | 296.34 | 0.42 | 0.14 | |
| 13 | MKEH | 293.87 | 0.5 | 0.17 | 0.2 |
| | 4π(PC)α-x,γ coinc | 293.87 | 0.5 | 0.17 | |
| 14 | NIST | 293.31 | 0.53 | 0.18 | -0.8 |
| | 4π(LS)α-x,γ anticoinc | 293.31 | 0.53 | 0.18 | |
| 15 | NMIJ | 293.96 | 0.7 | 0.25 | 0.3 |
| | 4π(PC)α-x,γ coinc | 293.96 | 0.7 | 0.25 | |
| 16 | NMISA ^(b) | 294.90 | 0.27 | 0.09 | 4.1 |
| | 4π(LS)α-x,γ coinc | 294.90 | 0.27 | 0.09 | |
| 17 | NPL ^(c) | 293.58 | 0.5 | 0.17 | -0.3 |
| | 4π(PC)α-x,γ coinc | 293.58 | 0.5 | 0.17 | |
| | 4π(PC)α-x,γ coinc DCC | 293.60 | 0.5 | 0.17 | |
| 18 | PTB | 293.35 | 0.53 | 0.18 | -0.8 |
| | 4π(PC)α-x,γ coinc | 293.70 | 0.9 | 0.31 | |
| | 4πmix-LSC | 292.80 | 0.9 | 0.31 | |
| | α-DSA-PIPS | 293.60 | 1.0 | 0.34 | |
| 19 | RC | 293.71 | 0.44 | 0.15 | -0.1 |
| | TDCR | 293.80 | 0.5 | 0.17 | |
| | 4π(LS)α-x,γ coinc | 293.40 | 0.9 | 0.31 | |
| 20 | SMÚ ^(a) | 296.6 | 3.6 | 1.2 | 0.8 |
| | 4πx,γ-IC | 296.6 | 3.6 | 1.2 | |
| 21 | VNIIM | 293.46 | 0.26 | 0.09 | -1.2 |
| | 4π(PC)α-x,γ coinc | 293.34 | 0.35 | 0.12 | |
| | α-DSA | 293.64 | 0.44 | 0.15 | |

^(a)Secondary standardisation method, not included in calculation of PMM

^(b)Excluded from calculation of PMM on statistical grounds

^(c)DCC = digital coincidence counting (both NPL measurements are identical, except for digital versus classical electronic signal processing)

Fig. 12 Updated (unofficial) version of the ‘draft A’ results overview of the 2003 CCRI(II)-K2.Am-241 key comparison exercise



as distributed to the participants, and (3) an official table of mean values for each participating laboratory [6]. Combining this information and updating the names of the NMIs to their current version, an unofficial new version of the ‘draft A’ plot is presented in Fig. 12. The most commonly used methods are coincidence counting techniques, liquid scintillation counting, and alpha-particle counting at a small solid angle. Each NMI provided a single official result, for which they independently chose which and how partial results were weighted in their mean value.

Since there is no objective arbiter in interlaboratory comparisons at the highest level of metrological accuracy, the Key Comparison Reference Value (KRCV) is a consensus value derived from the activity concentration values provided by the participating laboratories. This is calculated from a PMM using a default setting of the power depending on the number of data included in the mean [47]. Three data were not weighted in because they were obtained with secondary standardisation techniques (see Table 2) and three more values were excluded for being recognised as potential outliers by the default statistical criterion [47]. In calculating the degree of equivalence (DoE) of each laboratory (based on expanded uncertainty with $k=2$), or the related ζ -score (based on standard uncertainty or $k=1$) in Table 2, the correlation of the PMM with each weighted value is compensated for [46, 47]. The resulting PMM for the ^{241}Am activity per unit mass is $293.75 (10) \text{ kBq g}^{-1}$.

The PomPlot [49–51] in Fig. 13 allows for a quick assessment of the quality of the key comparison. It shows convincing consistency among the 16 data that contributed to the

PMM, with a χ^2 value of 0.85; 13 data have a zeta score of less than unity, which shows up as a dot within the green lines of the PomPlot, and 3 data are in the zone between green and blue ($1 < \zeta < 2$). (In the original PomPlot [49, 50], the straight lines refer to the z-value, whereas in the version introduced by Simon Jerome et al. [51], the uncertainty of the reference value is taken into account to show the ζ -score.) An additional PomPlot of all partial results in Fig. 14 demonstrates again the consistency among the primary techniques. With exclusion of three potential ‘outliers’, this is a rare case in which the standard deviation of the data set is smaller than expected from the stated uncertainties ($\chi^2=0.80$).

Conclusions

The JRC obtained consistent results for the activity standardisation of ^{241}Am in solution, using six primary standardisation methods. The relative uncertainty on the mean value, estimated as 0.054%, is arguably the lowest ever reported on an absolute activity measurement. It is consistent with the mean value obtained from 21 laboratories participating to the 2003 CCRI(II)-K2.Am-241 key comparison exercise. PomPlots witness that international equivalence of ^{241}Am activity standards has been convincingly demonstrated. Equivalence of standards does not imply identity, but it ensures statistical consistency in the presence of measurement uncertainty [1].

Fig. 13 PomPlot of the 2003 CCRI(II)-K2.Am-241 key comparison outcome. Empty symbols indicate secondary standardisation measurements not included in the reference value. The red dot indicates JRC's result. The symbols D and u refer to the deviation of results from the reference value and the stated standard uncertainty, respectively, whereas S represents a typical uncertainty per datum as defined in the PMM method [47]

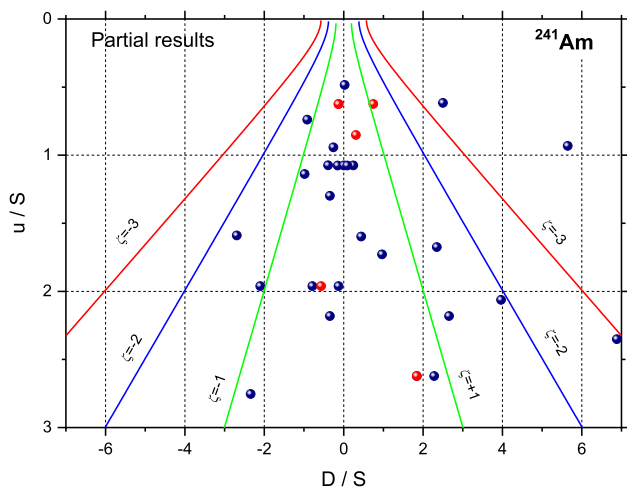
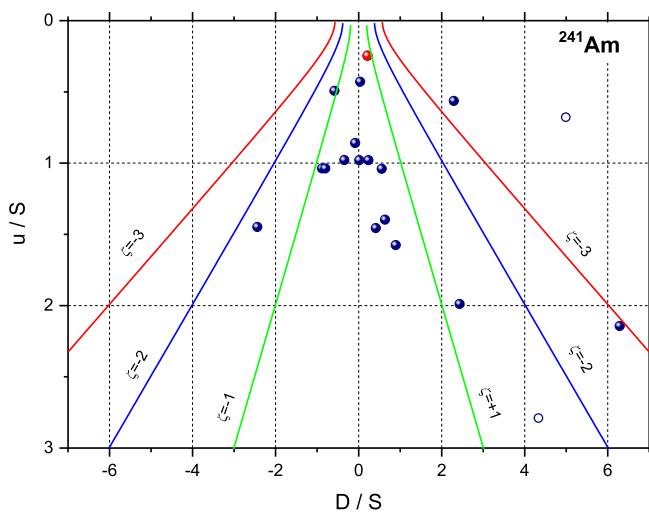


Fig. 14 PomPlot of the partial results obtained with primary methods in the 2003 CCRI(II)-K2.Am-241 key comparison. The red dots indicate JRC's partial results, of which two dots overlap at the top centre. The symbols D and u refer to the deviation of results from the reference value and the stated standard uncertainty, respectively, whereas S represents a typical uncertainty per datum as defined in the PMM method [47]

Acknowledgements The authors gratefully acknowledge the preparatory work by Dr Guy Ratel of the BIPM on collating all results from the key comparison in a 'draft A' overview graph and the support by Dr Krzysztof Pelczar who skilfully extracted data from the pdf file with the 'draft A' key comparison results.

Open Access This article is licensed under a Creative Commons Attribution 4.0 International License, which permits use, sharing, adaptation, distribution and reproduction in any medium or format, as long as you give appropriate credit to the original author(s) and the source, provide a link to the Creative Commons licence, and indicate if changes were made. The images or other third party material in this article are included in the article's Creative Commons licence, unless indicated otherwise in a credit line to the material. If material is not included in



the article's Creative Commons licence and your intended use is not permitted by statutory regulation or exceeds the permitted use, you will need to obtain permission directly from the copyright holder. To view a copy of this licence, visit <http://creativecommons.org/licenses/by/4.0/>.

References

1. Woods MJ, Reher DFG, Ratel G (2000) Equivalence in radionuclide metrology. *Appl Radiat Isot* 52:313–318
2. Pommé S (2007) Methods for primary standardization of activity. *Metrologia* 44:S17–S26
3. Ratel G (2007) The Système International de Référence and its application in key comparisons. *Metrologia* 44:S7–S16
4. Michotte C et al (2021) Final report of the new BIPM comparison BIPM..RI(II)-K1Tb-161 of activity measurements of the radionuclide ^{161}Tb including the 2019 result of the IRA(Switzerland). *Metrol Tech Suppl* 58:06009
5. BIPM, KCDB (key comparison database), <https://www.bipm.org/kcdb/>
6. Ratel G, Michotte C, Johansson L, Judge S, Kharitonov IA (2007) Update of the BIPM comparison BIPM.RI(II)-K1.Am-241 of activity measurements of the radionuclide ^{241}Am to include the 2006 VNIIM result, links for the international 2003 CCRI(II)-K2.Am-241 comparison and links for the 2006 regional comparison COOMET.RI(II)-K2.Am-241G. *Metrol Tech Suppl* 44:06007
7. Johansson L, Altizoglou T, Sibbens G, Pommé S, Denecke B (2003) Standardisation of ^{238}Pu using four methods of measurement. *Nucl Instr Meth A* 505:699–706
8. Johansson L, Altizoglou T, Sibbens G, Denecke B, Reher DFG (2003) Six direct methods for standardisation of ^{152}Eu . *Nucl Instr Meth A* 508:378–387
9. Pommé S, Altizoglou T, Van Ammel R, Sibbens G (2005) Standardisation of ^{125}I using seven techniques for radioactivity measurement. *Nucl Instr Meth A* 544:584–592
10. Decay Data Evaluation Project (2004–2021) DDEP Monographie BIPM-5—Table of Radionuclides <http://www.inhb.fr/nucle-ar-data/nuclear-data-table/> Accessed from 11 June 2021
11. Pommé S, Paepen J, Marouli M (2019) Conversion electron spectroscopy of the 5954 keV transition in ^{241}Am alpha decay. *Appl Radiat Isot* 153:108848
12. Pommé S (2016) When the model doesn't cover reality: examples from radionuclide metrology. *Metrologia* 53:S55–S64

13. Sibbens G, Altitzoglou T (2007) Preparation of radioactive sources for radionuclide metrology. *Metrologia* 44:S71–S78
14. Denecke B, Sibbens G, Szabo T, Hult M, Persson L (2000) Improvements in quantitative source preparation. *Appl Radiat Isot* 52:351–355
15. Pommé S (2015) Typical uncertainties in alpha-particle spectrometry. *Metrologia* 52:S146–S155
16. Denecke B (1994) Absolute activity measurements with the windowless 4π -CsI(Tl)-sandwich spectrometer. *Nucl Instrum Meth A* 339:92–98
17. de Jonghe S (1980) CBNM (JRC) Internal Report GE/TN/DE/60/80
18. Pommé S, Fitzgerald R, Keightley J (2015) Uncertainty of nuclear counting. *Metrologia* 52:S3–S17
19. Pommé S, Denecke B, Alzetta J-P (1999) Influence of pileup rejection on nuclear counting, viewed from the time-domain perspective. *Nucl Instrum Meth A* 426:564–582
20. Pommé S (2008) Cascades of pile-up and dead time. *Appl Radiat Isot* 66:941–947
21. Thiam C, Bobin C, Maringer FJ, Peyres V, Pommé S (2015) Assessment of the uncertainty budget associated with $4\pi\gamma$ counting. *Metrologia* 52:S97–S107
22. Pommé S (2009) Detection efficiency calculation for photons, electrons and positrons in a well detector; Part I: analytical model. *Nucl Instrum Meth A* 604:584–591
23. Pommé S, Sibbens G, Vidmar T, Camps J, Peyres V (2009) Detection efficiency calculation for photons, electrons and positrons in a well detector; Part II: analytical model versus simulations. *Nucl Instrum Meth A* 606:501–507
24. Pommé S, Camps J, Sibbens G, Spasova Y (2009) Some modifications to Sima's model for total efficiency calculation of well-type photon detectors. *J Radioanal Nucl Chem* 281:143–147
25. Pommé S (2012) STEFFY – Software for calculation of nuclide-specific total counting efficiency in well-type γ -ray detectors. *Appl Radiat Isot* 70:2070–2074
26. Lourenço V, Bobin C (2015) Weighing uncertainties in quantitative source preparation for radionuclide metrology. *Metrologia* 52:S18–S29
27. Pommé S (2015) The uncertainty of the half-life. *Metrologia* 52:S51–S65
28. Pommé S et al (2018) Is decay constant? *Appl Radiat Isot* 134:6–12
29. Pommé S, Stroh H, Van Ammel R (2019) The ^{55}Fe half-life measured with a pressurised proportional counter. *Appl Radiat Isot* 148:27–34
30. Denecke B, Grosse G, Szabo T (1998) Gain stabilisation of gas-flow proportional counters. *Appl Radiat Isot* 49:1117–1121
31. NIST, ASTAR program for the calculation of stopping powers. <https://physics.nist.gov/PhysRefData/Star/Text/ASTAR.html>
32. International Commission on Radiation Units and Measurements (1994) Particle Counting in Radioactivity Measurements, ICRU Report 52 (Maryland, USA) pp 80
33. Bobin C (2007) Primary standardization of activity using the coincidence method based on analogue instrumentation. *Metrologia* 44:S27–S31
34. Keightley J, Park TS (2007) Digital coincidence counting for radionuclide standardization. *Metrologia* 44:S32–35
35. Fitzgerald R, Bailat C, Bobin C, Keightley JD (2015) Uncertainties in $4\pi\beta\text{-}\gamma$ coincidence counting. *Metrologia* 52:S86–S96
36. Pommé S (2015) The uncertainty of counting at a defined solid angle. *Metrologia* 52:S73–S85
37. Pommé S, Sibbens G (2008) Alpha-particle counting and spectrometry in a primary standardisation laboratory. *Acta Chim Slov* 52:111–119
38. Pommé S, Johansson L, Sibbens G, Denecke B (2001) A new algorithm for the solid angle calculation applied in alpha-particle counting. Internal Report IRMM (JRC), GE/R/RN/08/2001, pp. 33
39. Marouli M, Pommé S (2019) Automated optical distance measurements for counting at a defined solid angle. *Appl Radiat Isot* 153:108821
40. Pommé S (2004) A complete series expansion of Ruby's solid-angle formula. *Nucl Instrum Meth A* 531:616–620
41. Pommé S, Paepen J (2007) A series expansion of Conway's generalised solid-angle formulas. *Nucl Instrum Methods A* 579:272–274
42. Pommé S, Johansson L, Sibbens G, Denecke B (2003) An algorithm for the solid angle calculation applied in alpha-particle counting. *Nucl Instrum Methods A* 505:286–289
43. Sibbens G, Pommé S, Johansson L, Denecke B (2003) Tailoring solid angle calculations to the actual radioactivity distribution of planar sources. *Nucl Instrum Methods A* 505:277–281
44. Van Ammel R, Eykens S, Eykens R, Pommé S (2011) Preparation of drop-deposited quantitative uranium sources with low self-absorption. *Nucl Instrum Meth A* 652:76–78
45. Pommé S, Spasova Y (2008) A practical procedure for assigning a reference value and uncertainty in the frame of an interlaboratory comparison. *Accred Qual Assur* 13:83–89
46. Pommé S (2012) Determination of a reference value, associated standard uncertainty and degrees of equivalence —for CCRI(II) key comparison data. JRC Scientific and Policy Reports EUR 25355 EN (EUR—Scientific and Technical Research Series) (<https://doi.org/10.2787/61338> 2012)
47. Pommé S, Keightley J (2015) Determination of a reference value and its uncertainty through a power-moderated mean. *Metrologia* 52:S200–S212
48. Supplementary data to Ref. 47: Spreadsheet with PMM algorithm downloadable at the Metrologia website: <https://iopscience.iop.org/article/https://iopscience.iop.org/article/https://doi.org/10.1088/0026-1394/52/3/S200>
49. Pommé S (2006) An intuitive visualisation of intercomparison results applied to the KCDB. *Appl Radiat Isot* 64:1158–1162
50. Spasova Y, Pommé S, Wätjen U (2007) Visualisation of interlaboratory comparison results in PomPlots. *Accred Qual Ass* 12:623–627
51. Jerome S et al (2020) Half-life determination and comparison of activity standards of ^{231}Pa . *Appl Radiat Isot* 155:108837

Publisher's Note Springer Nature remains neutral with regard to jurisdictional claims in published maps and institutional affiliations.